frontiers | Frontiers in Oncology

TYPE Original Research
PUBLISHED 01 December 2022
DOI 10.3389/fonc.2022.828312

OPEN ACCESS

EDITED BY
Giuseppe Minniti,
University of Pittsburgh Medical Center, United States

REVIEWED BY
Fabiana Gregucci,
Ospedale Generale Regionale Francesco Miulli, Italy
Siyong Kim,
Virginia Commonwealth University, United States

*CORRESPONDENCE
Yong Yin
yinyongsd@126.com

†These authors have contributed equally to this work

SPECIALTY SECTION
This article was submitted to Radiation Oncology, a section of the journal Frontiers in Oncology

RECEIVED 03 December 2021
ACCEPTED 15 November 2022
PUBLISHED 01 December 2022

CITATION
Hou C, Yin H, Gong G, Wang L, Su Y, Lu J and Yin Y (2022) A novel approach for dose painting radiotherapy of brain metastases guided by mr perfusion images. *Front. Oncol.* 12:828312. doi: 10.3389/fonc.2022.828312

A novel approach for dose painting radiotherapy of brain metastases guided by mr perfusion images

Chuanke Hou[1†], Hanjing Yin[2†], Guanzhong Gong[2], Lizhen Wang[2], Ya Su[2], Jie Lu[2] and Yong Yin[2*]

[1]Department of Radiology, Beijing YouAn Hospital, Capital Medical University, Beijing, China, [2]Department of Radiation Physics, Shandong Cancer Hospital and Institute, Shandong First Medical University and Shandong Academy of Medical Sciences, Ji'nan, China

Purpose: To investigate the feasibility and dosimetric index features of dose painting guided by perfusion heterogeneity for brain metastasis (BMs) patients.

Methods: A total of 50 patients with single BMs were selected for this study. CT and MR simulation images were obtained, including contrast-enhanced T1-weighted images (T1WI+C) and cerebral blood flow (CBF) maps from 3D-arterial spin labeling (ASL). The gross tumor volume (GTV) was determined by fusion of CT and T1WI+C images. Hypoperfused subvolumes (GTV_H) with less than 25% of the maximum CBF value were defined as the dose escalation region. The planning target volume (PTV) and PTV_H were calculated from GTV and GTV_H respectively. The PTV_N was obtained by subtracting PTV_H from PTV, and conventional dose was given. Three kinds of radiotherapy plans were designed based on the CBF values. Plan 1 was defined as the conventional plan with an arbitrary prescription dose of 60 Gy for PTV. For dose painting, Plan 2 and Plan 3 escalated the prescription dose for PTV_H to 72 Gy based on Plan 1, but Plan 3 removed the maximum dose constraint. Dosimetric indices were compared among the three plans.

Results: The mean GTV volume was 34.5 (8.4-118.0) cm^3, and mean GTV_H volume was 17.0 (4.5-58.3) cm^3, accounting for 49.3% of GTV. Both conventional plan and dose painting plans achieved 98% target coverage. The conformity index of PTV_H were 0.44 (Plan1), 0.64 and 0.72 (Plan 2 and Plan 3, $P<0.05$). Compared to Plan 1, the $D_{2\%}$, $D_{98\%}$ and D_{mean} values of the PTV_H escalated by 20.50%, 19.32%, and 19.60% in Plan 2 and by 24.88%, 17.22% and 19.22% in Plan 3 respectively ($P<0.05$). In the three plans, the index of

achievement value for PTV_H was between 1.01 and 1.03 ($P<0.05$). The dose increment rates of Plan 2 and Plan 3 for each organs at risk (OARs) was controlled at 2.19% - 5.61% compared with Plan 1. The doses received by OARs did not significantly differ among the three plans ($P>0.05$).

Conclusions: BMs are associated with significant heterogeneity, and effective escalation of the dose delivered to target subvolumes can be achieved with dose painting guided by 3D-ASL without extra doses to OARs.

KEYWORDS

brain metastases, radiotherapy, dose painting, 3D-arterial spin labeling, subvolume

Introduction

Brain metastases (BMs) are the most common intracranial malignant tumors, and approximately 8-10% of tumor patients will develop BMs during their disease course (1). Approximately 30-50% of BMs patients die of uncontrolled and recurrent intracranial lesions (2). And large-volume BMs are highly heterogeneous due to their long growth cycle and complex blood supply (3, 4). Subvolumes with low cerebral blood flow (CBF) are hypoxic or potentially hypoxic areas, which are associated with radiation resistance (3). Ling et al. has proved that the tumor volume must be considered heterogeneous when assessing function and treatment response (5).

At present, radiotherapy (RT) is considered a curative-intent treatment for BMs patients primarily consisting of whole-brain radiotherapy (WBRT) and stereotactic radiosurgery (SRS) (6, 7). WBRT is suitable for multiple BMs and high-dose SRS plays an important role in treatment of small-volume BMs while it is limited for large-volume BMs (8). RT failure is usually manifested by insufficient local radiation doses and radiation-induced brain injury.

3D-arterial spin labeling (3D-ASL) perfusion imaging analyzes CBF parameters noninvasively and quantitatively and is independent of blood-brain barrier (BBB) damage (9). In addition, 3D-ASL has been widely used in clinical diagnosis, differential diagnosis and efficacy evaluation of brain tumors (9–11). Due to the tumor-specific characteristics of large-volume BMs, 3D-ASL is potentially promising for image-guided RT treatment planning with dose painting (12). Dose painting refers to the distribution of nonuniform radiation doses to target volumes according to functional or molecular images (13).

Increasing the doses to BMs can significantly improve the curative effect. Therefore, safe dose escalation for target subvolumes of BMs is crucial. This study therefore explored the feasibility of 3D-ASL-guided subvolume segmentation of BMs based on CBF map variation. In addition, we further studied the dosimetric indices of dose painting plans to provide additional reference for the formulation and modification of individualized RT to BMs patients.

Materials and methods

Patients

Fifty patients, namely, 29 males and 21 females (aged 33 - 74 years, with a median age of 57 years), with a single BMs who received RT were selected from July 2018 to September 2020. There were 33 cases of lung cancer, 9 of breast cancer, 4 of renal carcinoma, 2 of esophageal cancer and 2 of colon cancer. All patients were diagnosed with BMs with imaging and the maximum tumor cross-sectional diameter was more than 2 cm. The retrospective analysis of the medical records was approved by the Institutional Review Board of Shandong Cancer Hospital.

Computed Tomography and MR Simulation

CT simulation images (slice thickness = 3 mm; slice gap = 3 mm) were obtained by Brilliance Big Bore CT scanner (Philips, Netherlands). MR imaging was performed on 3.0 T Discovery 750 W MR scanner (GE Healthcare, USA) with the same head position as CT simulation. 3D-ASL and contrast-enhanced T1-weighted (T1WI+C) images were acquired using 3D volume scanning (field of view, FOV= 26 cm; matrix size = 256×256; slice thickness = 3 mm). For 3D-ASL images, the special acquisition conditions were as follows: repetition time (TR) = 5160ms; echo time (TE) = 11.5 ms; and postlabeling delay (PLD) = 2025 ms. David et al. pointed out that it is more reasonable to set the PLD of healthy people older than 70 years old and adult

clinical patients to around 2000ms (14). For T1WI+C images, TR = 8.5 ms; and TE = 3.2 ms. Gadopentetate dimeglumine was power-injected applying doses standardized by 0.2 mL/kg at 2 mL/s, and scan started 3 - 5 min after injection.

Target volume definition

CT and T1WI+C images were fused in MIM Maestro software (6.8.8, USA), and gross tumor volume (GTV) was defined as the region with high signal. The GTV was divided into hypoperfused (GTV_H), hyperperfused and nonperfused subvolumes based on CBF values (15). One-quarter of maximum CBF value was the junction of hypoperfused and hyperperfused subvolumes (16). Planning target volume (PTV) was designated as GTV plus a 5 mm margin, and 3 mm margins were added to the GTV_H to obtain PTV_H. Then, the PTV_N was obtained by subtracting the PTV_H from the PTV, which was given normal prescription dose. Schematic diagrams are shown in Figures 1, 2.

Treatment plans

Conventional and dose painting plans were implemented by intensity-modulated radiotherapy (IMRT) and simultaneous integrated boost (SIB) IMRT. These plans were designed using Eclipse (Version 15.6, Varian, USA). For larger tumors, with the most common doses being 27 Gy in 3 fractions and 30 Gy in 5 fractions applying with SRS based on NCCN (17). Preliminary results from a randomized phase II trial comparing dose-intensification with standard-dose IMRT for newly diagnosed glioblastoma demonstrate that a higher radiation dose improves overall survival (18). The tolerance dose for brain to a single course of RT is 60 Gy in 2 Gy daily fractions (19). And both the hypoxic areas of BMs have the same characteristics of RT resistance with glioblastoma, so we refer to the treatment plan of glioblastoma (20). Here, we set the prescription dose at 60 Gy and the elevated dose at 72 Gy (20). Boosting tumor subvolume may increase tumor control probability (TCP), and a moderate boost dose (120% -150%) to hypoxic areas is also beneficial to increase TCP (21, 22). The conventional plan (60 Gy) and the dose painting plan (72 Gy) were both set at 2 Gy/d in this study. The conventional plan, designated Plan 1, prescribed 60 Gy to PTV with a maximum dose (D_{max}) constraint of 66 Gy (110% of prescription dose). For dose painting, Plan 2 escalated the PTV_H to 72 Gy with a D_{max} constraint of 79 Gy (110% of prescription dose) based on Plan 1. Moreover, Plan 3 was designed depending on Plan 2 without D_{max} constraint.

The optimized parameters and dose constraints for organs at risk (OARs) among three plans were unified. OARs were restricted to the following doses: D_{max}<50 Gy for eye, D_{max}<54 Gy for optic nerve, $D_{max<}$ 8 Gy for lens, and D_{max}<54 Gy for brainstem.

Dose calculation was performed in anisotropic analytical algorithm optimization mode (version 15.512) using 6 MV X-

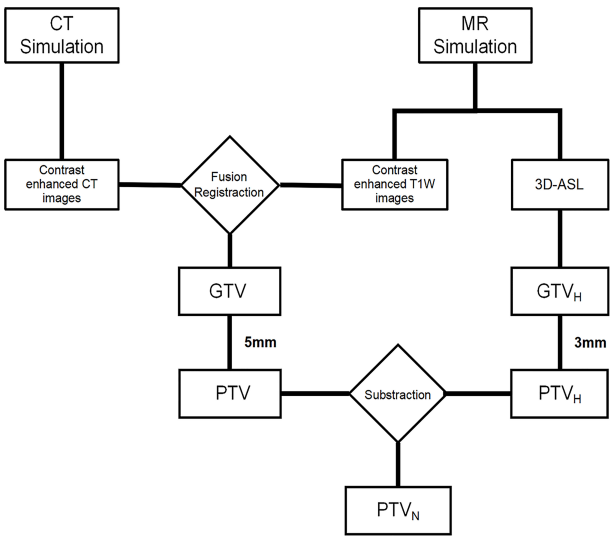

FIGURE 1
Target volume determination flow chart.

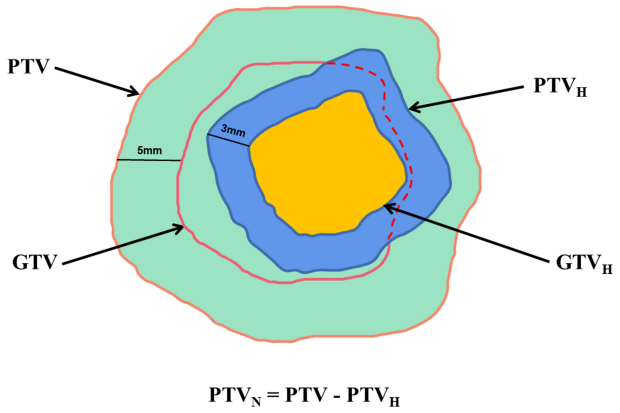

FIGURE 2
Illustration of the target volumes.

rays. The calculated grid was 2.5 mm×2.5 mm, and the prescription dose was acquired to cover 95% of the target volume.

Evaluation of plan dosimetric indices

For PTVs, the $D_{2\%}$, $D_{98\%}$ and D_{mean} (doses to 2%, 98% and 50% volume of the PTV, respectively) were the maximum, minimum and mean dose, respectively. The D_{max} values of eyeballs, optic nerves, lenses and brainstem were compared. Furthermore, the target coverage, conformity index (CI) and index of achievement (IOA) were calculated. The proposed IOA is formulated as the volume-weighted average of the deviation between prescription dose and planned dose (23).

The formulas for calculating CI and IOA are as follows:

$$CI = \frac{V_{t,ref}}{V_t} \times \frac{V_{t,ref}}{V_{ref}};$$

$$IOA = 1 + \sqrt{\sum_{K=1}^{K}\sum_{j=1}^{j}\left[\left(\frac{D_j - D_{K,RX}}{D_{K,RX}}\right)^2 \times \frac{dDVH_{PTV(K)}(D_j)}{V_{PTV(K)}}\right]}$$

where V_t represents the PTVs, $V_{t,ref}$ represents the target volume covered by prescription dose, and V_{ref} represents the volume covered by prescription dose. where K is the total number of PTVs, $D_{K,RX}$ is the prescription dose for the Kth PTV, and $V_{PTV(K)}$ is the volume of the kth PTV, where j is the total number of volumes, D_j is the jth volumes dose value, and $dDVH_{PTV(K)}(D_j)$ is the absolute volume (cc) of the jth dose volume in the kth PTV.

CI near 1 indicates that region receiving the reference dose closely matches the shape of the target region (24). IOA have values equal to or greater than 1 and value farther from 1 indicates greater dissimilarity (23).

Data statistics

Statistical analysis was performed using SPSS Statistics Version 22.0 (IBMs, USA). Analysis of variance was used to evaluate the differences among the three plans. *F* value is used to evaluate the difference between groups. The larger the *F* is, the more significant the equation is, and the better the fitting degree is. The least significant difference was used in pairwise comparisons. All data are expressed as mean ± standard deviation ($\bar{x} \pm S$), and $P<0.05$ indicates a significant difference.

Results

Target volume and subvolume comparison

GTV had a volume range of 8.4-118.0 cm^3, with an average volume of 34.5 cm^3. And mean GTV_H was 17.0 (4.5-58.3) cm^3, accounting for 49.3% of the GTV. The PTV, PTV_H and PTV_N were 72.0 cm^3, 41.5 cm^3 and 30.5 cm^3, respectively. The ratios of PTV_H to PTV and PTV_N to PTV were 57.6% and 42.4%, respectively, as shown in Table 1 and Figure 3.

TABLE 1 Volume and volume ratio comparison.

Target volume	Volume (cm^3)	Volume ratio (%)
GTV	34.5 ± 21.7	—
GTV_H	17.0 ± 11.9	49.3
PTV	72.0 ± 34.7	—
PTV_H	41.5 ± 22.0	57.6
PTV_N	30.5 ± 18.6	42.4

10.3389/fonc.2022.828312

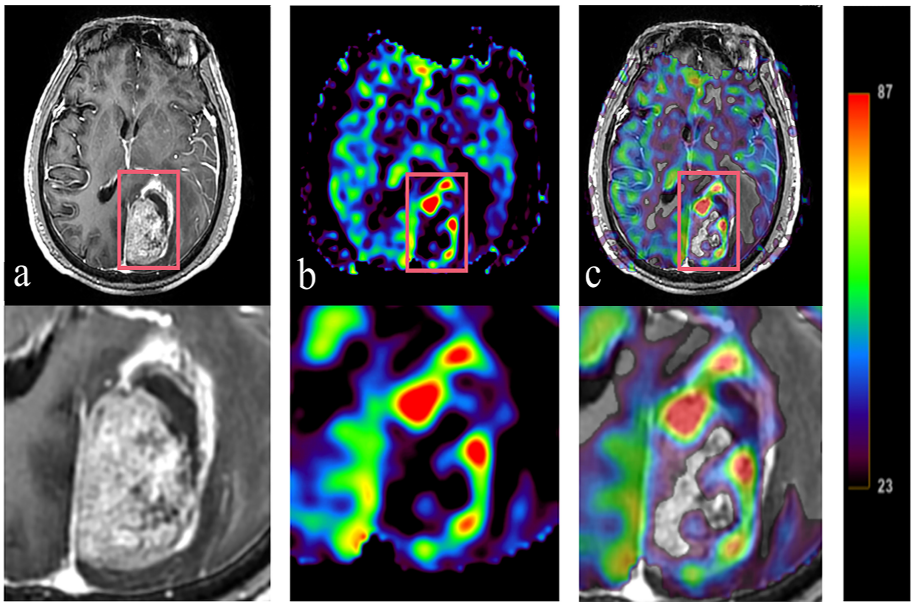

FIGURE 3
Tumor information is expressed T1WI+C and 3D-ASL images. A 61 year old BMs patient with primary colon carcinoma. According to the enhanced area shown in the T1WI+C images, 3D-ASL showed the uneven distribution of CBF in tumor. The hyperperfused subvolumes are mainly located on the left side of the enhanced edge, while the GTV_H and the enhanced area overlap in a large region. Moreover, the fusion image c shows this result better. **(A)** T1WI+C images; **(B)** 3D-ASL images; **(C)** 3D-ASL images fuse with T1WI+C images.

Target coverage, CI and IOA comparisons among three plans

As shown in Table 2, both conventional and dose painting plans achieved 98% target coverage, even though Plan 2 achieved coverage of PTV_H up to 99.90%. Compared with Plan 2, Plan 3 significantly increased the CI levels of PTV_H by 12.50% ($P< 0.05$). Owing to the use of targeted gradient doses instead of a group-based uniform dose, CI values of the PTV and PTV_N were lower in the dose painting plans than in the conventional plans. For PTV_H, the IOA values of the three plans were between 1.01 and 1.03 ($P< 0.05$). Meanwhile, the IOA values of PTV and PTV_N were between 1.01 and 1.10 ($P< 0.05$).

Comparison of the dosimetric indices among the three plans

The differences in all dosimetric indices of PTVs except $D_{2\%}$ were statistically significant ($P< 0.05$). Compared to those of Plan 1, the $D_{2\%}$, $D_{98\%}$ and D_{mean} of the PTV were increased by 20.18%, 8.34% and 18.38% in Plan2 and by 24.05%, 6.77% and

TABLE 2 Comparison of target coverage, CI and IOA among three plans.

Program		Plan1	Plan2	Plan3	*F*	*P*	P_{1-2}	P_{1-3}	P_{2-3}
Target coverage	PTV	99.60 ± 0.60	99.95 ± 0.13	99.86 ± 0.26	10.995	≤0.05	≤0.05	≤0.05	>0.05
	PTV_H	99.10 ± 5.19	99.90 ± 0.18	98.40 ± 1.47	2.895	>0.05	>0.05	>0.05	≤0.05
	PTV_N	99.15 ± 1.41	99.88 ± 0.34	99.76 ± 0.40	10.346	≤0.05	≤0.05	≤0.05	>0.05
CI	PTV	0.75 ± 0.07	0.54 ± 0.07	0.55 ± 0.07	144.791	≤0.05	≤0.05	≤0.05	>0.05
	PTV_H	0.44 ± 0.10	0.64 ± 0.14	0.72 ± 0.11	78.818	≤0.05	≤0.05	≤0.05	≤0.05
	PTV_N	0.28 ± 0.09	0.21 ± 0.07	0.21 ± 0.07	12.457	≤0.05	≤0.05	≤0.05	>0.05
IOA	PTV	1.02 ± 0.01	1.10 ± 0.03	1.09 ± 0.04	112.623	≤0.05	≤0.05	≤0.05	≤0.05
	PTV_H	1.03 ± 0.01	1.02 ± 0.01	1.01 ± 0.02	95.152	≤0.05	≤0.05	≤0.05	≤0.05
	PTV_N	1.01 ± 0.02	1.08 ± 0.03	1.06 ± 0.03	66.247	≤0.05	≤0.05	≤0.05	≤0.05

F and P were the results of analysis of variance; P_{1-2}, Plan 1 vs Plan 2; P_{1-3}, Plan 1 vs Plan 3; P_{2-3}, Plan 2 vs Plan 3.

17.00%, respectively, in Plan 3. The dosimetric indices above for PTV_H were increased by 20.50%, 19.32% and 19.60% in Plan 2, while those of Plan 3 were increased by 24.88%, 17.22% and 19.22%. Similarly, the dosimetric indices of PTV_N were increased in Plan 2 and Plan 3 (18.81%, 7.17%, 14.31%; 19.69%, 5.15%, 11.80%). Additionally, the $D_{2\%}$ values of PTVs showed increasing trends among three plans, while the increment rates of $D_{98\%}$ and D_{mean} for Plan 2 were higher than those for Plan 3, as shown in Table 3 and Figure 4.

There was no significant difference in D_{max} received by OARs between conventional and dose painting plans ($P > 0.05$). Nevertheless, the dose painting plans slightly increased the D_{max} of all OARs compared to Plan 1, while right eye increased by 5.61% to 0.50 Gy in Plan 3. The other OARs increased by less than 5.40% (2.19% - 5.30%), as shown in Table 4.

Discussion

This study demonstrated that BMs can be divided into high and low perfusion subvolumes based on 3D-ASL. We therefore presented a new method for assessing the clinical feasibility of dose painting plans directed by 3D-ASL for BMs. The results showed that the technique above can be completed feasibly without increasing the dose delivered to OARs which holds the potential to achieve better control of BMs than traditional RT treatment.

TABLE 3 Comparison of $D_{2\%}$、$D_{98\%}$ and D_{mean} among three plans.

Program		Plan1	Plan2	Plan3	*F*	*P*	P_{1-2}	P_{1-3}	P_{2-3}
PTV	$D_{2\%}$(Gy)	64.42 ± 0.37	77.42 ± 0.62	79.91 ± 2.28	1818.024	≤0.05	≤0.05	≤0.05	≤0.05
	$D_{98\%}$(Gy)	61.17 ± 0.66	66.27 ± 2.07	65.31 ± 2.25	112.920	≤0.05	≤0.05	≤0.05	≤0.05
	D_{mean}(Gy)	63.29 ± 0.19	74.92 ± 0.68	74.05 ± 0.84	5178.923	≤0.05	≤0.05	≤0.05	≤0.05
PTV_H	$D_{2\%}$(Gy)	64.38 ± 0.61	77.58 ± 0.52	80.40 ± 2.39	1727.402	≤0.05	≤0.05	≤0.05	≤0.05
	$D_{98\%}$(Gy)	61.74 ± 0.69	73.67 ± 0.34	72.37 ± 0.61	6660.500	≤0.05	≤0.05	≤0.05	≤0.05
	D_{mean}(Gy)	63.43 ± 0.19	75.86 ± 0.08	75.62 ± 0.29	58745.045	≤0.05	≤0.05	≤0.05	≤0.05
PTV_N	$D_{2\%}$(Gy)	64.39 ± 0.50	76.50 ± 1.19	77.07 ± 2.61	904.842	≤0.05	≤0.05	≤0.05	>0.05
	$D_{98\%}$(Gy)	60.55 ± 1.54	64.89 ± 1.83	63.67 ± 1.94	79.330	≤0.05	≤0.05	≤0.05	≤0.05
	D_{mean}(Gy)	63.05 ± 0.27	72.07 ± 0.71	70.49 ± 0.88	2551.806	≤0.05	≤0.05	≤0.05	≤0.05

F and P were the results of analysis of variance; P_{1-2}, Plan1 vs Plan2; P_{1-3}, Plan 1 vs Plan 3; P_{2-3}, Plan 2 vs Plan 3.

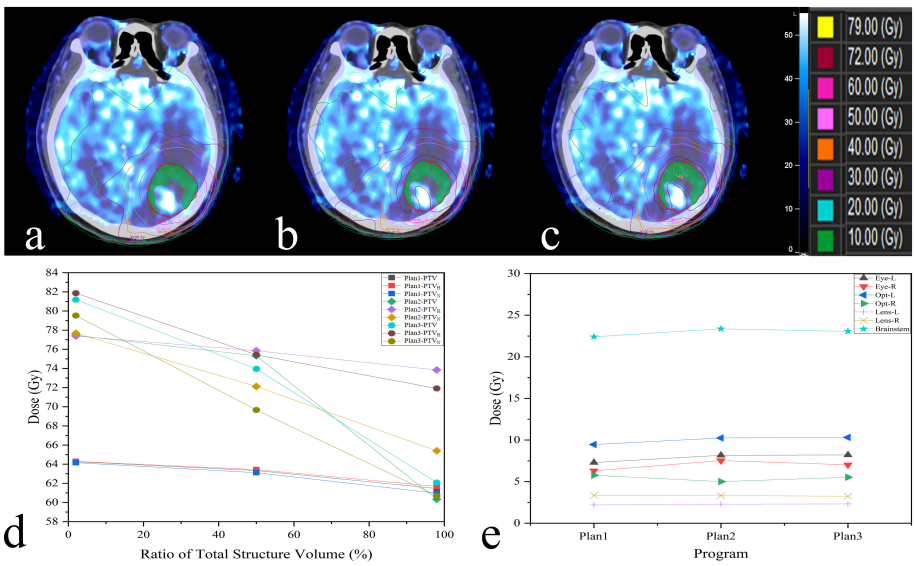

FIGURE 4
The difference among three plans is shown in this example (**A**:Plan1; **B**:Plan2; **C**:Plan3);. Display on axial slices for dose painting plan showing prescribed 72 Gy around PTV_H (green). The dosimetric indices $D_{2\%}$, $D_{98\%}$, Dmean and the dose received by OARs are also revealed in **(D, E)**.

10.3389/fonc.2022.828312

TABLE 4 Comparison of organs at risk among three plans.

Program	Eye-L (Dmax-Gy)	Eye-R (Dmax-Gy)	Optic nerve-L (Dmax-Gy)	Optic nerve-R (Dmax-Gy)	Lens-L (Dmax-Gy)	Lens-R (Dmax-Gy)	Brainstem (Dmax-Gy)
Plan1	8.74 ± 9.06	8.92 ± 9.99	8.36 ± 12.02	7.36 ± 9.39	2.31 ± 1.54	2.07 ± 1.54	18.68 ± 12.97
Plan2	8.97 ± 8.97	9.39 ± 10.19	8.62 ± 12.21	7.66 ± 9.77	2.37 ± 1.59	2.14 ± 1.55	19.09 ± 13.23
Plan3	8.98 ± 8.75	9.42 ± 10.15	8.67 ± 12.29	7.75 ± 9.83	2.40 ± 1.68	2.15 ± 1.53	19.14 ± 13.30
F	0.012	0.039	0.009	0.023	0.038	0.049	0.018
P	>0.05	>0.05	>0.05	>0.05	>0.05	>0.05	>0.05
$\%_{(1\text{-}2)}$	2.63	5.27	3.11	4.08	2.60	3.38	2.19
$\%_{(1\text{-}3)}$	2.75	5.61	3.71	5.30	3.90	3.86	2.46
$\%_{(2\text{-}3)}$	0.11	0.32	0.58	1.17	1.27	0.47	0.26
$P_{1\text{-}2}$	>0.05	>0.05	>0.05	>0.05	>0.05	>0.05	>0.05
$P_{1\text{-}3}$	>0.05	>0.05	>0.05	>0.05	>0.05	>0.05	>0.05
$P_{2\text{-}3}$	>0.05	>0.05	>0.05	>0.05	>0.05	>0.05	>0.05

F and P were the results of analysis of variance; $\%_{(1\text{-}2)}$, % increment between Plan 1 and Plan 2; $\%_{(1\text{-}3)}$, % increment between Plan 1 and Plan 3; $\%_{(2\text{-}3)}$, % increment between Plan 2 and Plan 3; $P_{1\text{-}2}$, Plan 1 vs Plan 2; $P_{1\text{-}3}$, Plan 1 vs Plan 3; $P_{2\text{-}3}$, Plan 2 vs Plan 3.

BMs are significant health problems whose incidence is increasing, and the median survival time is only 1-2 months without treatment (1, 25). Numerous studies have indicated that increasing the radiation dose significantly improves the local control of BMs, and some patients have achieved long-term survival (26, 27). Therefore, RT is an irreplaceable treatment for BMs. However, increasing radiation dose, particularly to vascular endothelial cells and glial cells, is associated with elevated toxicity and reduced tolerance to treatment (28). Thus, dose escalation without guidance is relevant to high risk of radiation induced brain injury.

Some studies have shown that BMs are highly heterogeneous according to their pathological sources or even sites of pathological origin (29). Brown et al. proposed that the blood flow in hypoxic tissue is slower than that in normal tissue and cannot satisfy the oxygen requirement of rapidly proliferating tumor cells because of highly irregular tumor vessels, arteriovenous shunts, blind ends, an incomplete basement membrane of vascular epithelial cells and other factors (30). Due to the uneven distribution of blood flow and cancer cells, BMs appear as radiation-sensitive regions with high perfusion, hypoxic radiation-resistant regions with low perfusion, and necrotic regions. Furthermore, the isoeffective dose can be up to three times higher under hypoxic conditions than under normoxic conditions (31). However, the group-based uniform dose given under a conventional plan cannot guarantee a sufficient dose for radiation-resistant regions, which eventually leads to further tumor progression and recurrence; local control failures are not uncommon under conventional treatment.

Dose escalation according to heterogeneity is essential, and primary task is to determine the tumor target subvolume with biological images. Perfusion-weighted MR can be used for quantitative analysis of blood flow parameters (9, 11, 16, 32). The noninvasive technology 3D-ASL reflects angiogenesis and other functional features of tumor microvascular system, rather than reflecting only morphology as CT and conventional MR (9). The amount of blood in one slice was evaluated by measuring the signal reduction after arterial blood saturation with radio frequency pulse. Therfore, ASL observe cerebral perfusion without using contrast agent, and has good safety and repeatability. Yukie et al. demonstrated that the area under the curve value of ASL for the recognition of hypoxic areas reached 0.83 based on the hypoxic tracer ^{18}F-fluoromisonidazole (10). Our previous studies also demonstrated that the CBF variations in brain tissue and BMs following radiation dose gradients could be quantified by 3D-ASL. In this paper, 49.3% of the GTV was within a region of low CBF which showed that subvolume segmentation based on CBF map using 3D-ASL is feasible (33).

A major concern regarding the implementation of dose escalation for specific subvolumes can be solved by dose painting which aims to improve tumor control without adding doses to OARs (34). Dose painting guided by positron emission computed tomography (PET) has been widely studied in head and neck tumors, but the application of PET is indisputably limited at present because of its invasiveness and high price (35, 36). Perfusion technique has been proved to be used to improve radiotherapy regimens and provide more biological information (37).Thus, in the present study, dose painting was used to achieve dose escalation in hypoperfused subvolumes that were recognized and segmented by 3D-ASL. The results demonstrated that compered those of Plan 1, the $D_{2\%}$, $D_{98\%}$ and D_{mean} of the PTV_H were increased by 20.50%, 19.32% and 19.60% in Plan 2, while those of Plan 3 were increased by 24.88%, 17.22% and

19.22%. Compared to the conventional plans of 60 Gy, the dose painting plans significantly increased the dosimetric indices. However, there were two trends. On the one hand, the maximum dose of PTVs all showed increasing trends among three plans. On the other hand, the constrained dose painting plans had better average and minimum doses than the other two plans, and this was the case for all PTVs. Thorwarth et al. noted that dose of up to 82 Gy may be applied to head and neck tumors without increasing toxicity, but constraints for normal tissue were not stated in their work (38). Our results indicated that the dose delivered to OARs was increased less than 4.10% (2.19%-4.08%) except for the right eye (5.27%; 0.47 Gy) when the prescription dose of PTV_H was increased by 20% in Plan2. Undoubtedly, the absolute dose was still far below the dose constraint. In addition, the constrained dose painting plans outperformed the unconstrained plans in terms of OARs protection.

Both conventional and dose painting plans achieved target coverage of more than 98%. Likewise, the constrained dose painting plans had better target coverage than unconstrained and conventional plans. Chang et al. pointed out that reducing the uniformity of radiation dose is beneficial for dose escalation and OAR protection (35). The IOA values of different PTVs in three plans are less than or equal to 1.10, which indicates that good targeted dose distribution can be achieved. Meanwhile, it is necessary to confirm CI because the shape of subvolumes defined by perfusion is often irregular. In this work, CI of the PTV_H was effectively guaranteed through the dose painting plans, which further proved the feasibility of our experimental method.

There are still some limitations in this study. First, PLD is one of the important parameters for accurate evaluation of CBF. However, in practice, it is difficult to ensure that PLD is set according to the specific conditions of patients to adapt to the arrival time of labeled arterial blood. Second, the effect of dose painting plans for BMs still needs to be confirmed in clinical practice. Relevant research is under way.

Conclusions

In summary, CBF maps based on 3D-ASL could be used for guiding subvolumes segmentation. Dose painting guided by different CBF variations offeres a novel approach for BMs RT. Safe dose escalation without additional radiation doses to OARs provides an effective individualized dose painting strategy for BMs patients.

Data availability statement

The raw data supporting the conclusions of this article will be made available by the authors, without undue reservation.

Ethics statement

The studies involving human participants were reviewed and approved by Institutional Review Board of the Shandong Cancer Hospital. Written informed consent for participation was not required for this study in accordance with the national legislation and the institutional requirements.

Author contributions

CH, HY, and YY designed the study and wrote the initial draft of the manuscript. GG contributed to the design of the study and the analysis and interpretation of data and assisted in the preparation of the manuscript. LW, YS, and JL contributed to data collection and interpretation, and critically reviewed the manuscript. All authors contributed to the article and approved the submitted version.

Funding

This work was supported by Key Support Program of Natural Science Foundation of Shandong Province (Grant No. ZR2019LZL017), the Taishan Scholars Project of Shandong Province (Grant No. ts201712098) and National Key Research and Development Program of China (Grant No. 2017YFC0113202).

Acknowledgments

We gratefully acknowledge Qingtao Qiu for his support with text proofing.

Conflict of interest

The authors declare that the research was conducted in the absence of any commercial or financial relationships that could be construed as a potential conflict of interest.

Publisher's note

References

1. Chamberlain MC, Baik CS, Gadi VK, Bhatia S, Chow LQ. Systemic therapy of brain metastases: Non-small cell lung cancer, breast cancer, and melanoma. *Neuro Oncol* (2017) 19(1):i1–i24. doi: 10.1093/neuonc/now197

2. Achrol AS, Rennert RC, Anders C, Soffietti R, Ahluwalia MS, Nayak L, et al. Brain metastases. *Nat Rev Dis Primers* (2019) 5:5. doi: 10.1038/s41572-018-0055-y

3. Lee CT, Boss MK, Dewhirst MW. Imaging tumor hypoxia to advance radiation oncology. *Antioxid Redox Signal* (2014) 21:313–37. doi: 10.1038/s41571-019-0320-3

4. Mahmood F, Hjorth Johannesen H, Geertsen P, Hansen RH. Diffusion MRI outlined viable tumour volume beats GTV in intra-treatment stratification of outcome. *Radiother Oncol* (2020) 144:121–6. doi: 10.1016/j.radonc.2019.11.012

5. Ling CC, Humm J, Larson S, Amols H, Fuks Z, Leibel S, et al. Towards multidimensional radiotherapy (MD-CRT): Biological imaging and biological conformality. *Int J Radiat Oncol Biol Phys* (2000) 47:551–60. doi: 10.1016/s0360-3016(00)00467-3

6. Xin Y, Guo WW, Yang CS, Cui HJ, Hu KW. Meta-analysis of whole-brain radiotherapy plus temozolomide compared with whole-brain radiotherapy for the treatment of brain metastases from non-small-cell lung cancer. *Can Med* (2018) 7 (4):981–90. doi: 10.1002/cam4.1306

7. Hughes RT, Masters AH, McTyre ER, Farris MK, Chung C, Page BR, et al. Initial SRS for patients with 5 to 15 brain metastases: Results of a multi-institutional experience. *Int J Radiat Oncol Biol Phys* (2019) 104:1091–8. doi: 10.1016/j.ijrobp.2019.03.052

8. Suh JH, Kotecha R, Chao ST, Ahluwalia MS, Sahgal A, Chang EL. Current approaches to the management of brain metastases. *Nat Rev Clin Oncol* (2020) 17:279–99. doi: 10.1038/s41571-019-0320-3

9. Wells JA, Thomas DL, Saga T, Kershaw J, Aoki I. MRI Of cerebral microvascular flow patterns: A multi-direction diffusion-weighted ASL approach. *J Cereb Blood Flow Metab* (2017) 37(6):2076–83. doi: 10.1177/0271678X16660985

10. Shimizu Y, Kudo K, Kameda H, Harada T, Fujima N, Toyonaga T, et al. Prediction of hypoxia in brain tumors using a multivariate model built from MR imaging and f-fluorodeoxyglucose accumulation data. *Magn Reson Med Sci* (2020) 19:227–34. doi: 10.2463/mrms.mp.2019-0049

11. Choi YJ, Kim HS, Jahng GH, Kim SJ, Suh D. Pseudoprogression in patients with glioblastoma: Added value of arterial spin labeling to dynamic susceptibility contrast perfusion MR imaging. *Acta Radiol* (2013) 54(4):448–54. doi: 10.1177/0284185112474916

12. Bentzen SM, Gregoire V. Molecular imaging-based dose painting: A novel paradigm for radiation therapy prescription. *Semin Radiat Oncol* (2011) 21:101–10. doi: 10.1016/j.semradonc.2010.10.001

13. Bentzen SM. Theragnostic imaging for radiation oncology: Dose-painting by numbers. *Lancet Oncol* (2005) 6:112–7. doi: 10.1016/S1470-2045(05)01737-7

14. Alsop DC, Detre JA, Golay X, Günther M, Hendrikse J, Hernandez-Garcia L, et al. Recommended implementation of arterial spin-labeled perfusion MRI for clinical applications: A consensus of the ISMRM perfusion study group and the European consortium for ASL in dementia. *Magn Reson Med* (2015) 73:102–16. doi: 10.1002/mrm.25197

15. Hou C, Gong G, Wang L, Su Y, Lu J, Yin Y. A study of dose painting with IMRT guided by perfusion-weighted magnetic resonance imaging for brain metastases. (2020). doi: 10.21203/rs.3.rs-131837/v1

16. Li C, Yan JL, Torheim T, McLean MA, Boonzaier NR, Zou J, et al. Low perfusion compartments in glioblastoma quantified by advanced magnetic resonance imaging and correlated with patient survival. *Radiother Oncol* (2019) 134:17–24. doi: 10.1016/j.radonc.2019.01.008

17. Nabors LB, Portnow J, Ahluwalia M, Baehring J, Brem H, Brem S, et al. Central nervous system cancers, version 3.2020, NCCN clinical practice guidelines in oncology. *J Natl Compr Canc Netw* (2020) 18(11):1537–70. doi: 10.6004/jnccn.2020.0052

18. Gondi V, Pugh S, Tsien C, Chenevert T, Gilbert M, Omuro A, et al. Radiotherapy (RT) dose-intensification (DI) using intensity-modulated RT (IMRT) versus standard-dose (SD) RT with temozolomide (TMZ) in newly diagnosed glioblastoma (GBM): Preliminary results of NRG oncology BN001. *Int J Radiat Oncol Biol Phys* (2020) 108:3. doi: 10.1016/j.ijrobp.2020.07.2109

19. Marks JE, Baglan RJ, Prassad SC, Blank WF. Cerebral radionecrosis: Incidence and risk in relation to dose, time, fractionation and volume. *Int J Radiat Oncol Biol Phys* (1981) 7:243–52. doi: 10.1016/0360-3016(81)90443-0

20. Ken S, Vieillevigne L, Franceries X, Simon L, Supper C, Lotterie JA, et al. Integration method of 3D MR spectroscopy into treatment planning system for glioblastoma IMRT dose painting with integrated simultaneous boost. *Radiat Oncol* (2013) 8:1. doi: 10.1186/1748-717X-8-1

21. Tomé WA, Fowler JF. Selective boosting of tumor subvolumes. *Int J Radiat Oncol Biol Phys* (2000) 48(2):593–9. doi: 10.1016/s0360-3016(00)00666-0

22. Popple RA, Ove R, Shen S. Tumor control probability for selective boosting of hypoxic subvolumes, including the effect of reoxygenation. *Int J Radiat Oncol Biol Phys* (2002) 54(3):921–7. doi: 10.1016/s0360-3016(02)03007-9

23. Park YK, Park S, Wu HG, Kim S. A new plan quality index for dose painting radiotherapy. *J Appl Clin Med Phys* (2014) 15(4):4941. doi: 10.1120/jacmp.v15i4.4941

24. Paddick I. A simple scoring ratio to index the conformity of radiosurgical treatment plans. Technical note. *J Neurosurg* (2000) 93 Suppl (3):219–22. doi: 10.3171/jns.2000.93.supplement

25. Bray F, Ferlay J, Soerjomataram I, Siegel RL, Torre LA, Jemal A. Global cancer statistics 2018: GLOBOCAN estimates of incidence and mortality worldwide for 36 cancers in 185 countries. *CA Cancer J Clin* (2018) 68:394–424. doi: 10.3322/caac.21492

26. Rades D, Kieckebusch S, Lohynska R, Veninga T, Stalpers LJ, Dunst J, et al. Reduction of overall treatment time in patients irradiated for more than three brain metastases. *Int J Radiat Oncol Biol Phys* (2007) 69:1509–13. doi: 10.1016/j.ijrobp.2007.05.014

27. Zhuang QY, Li JL, Lin FF, Lin XJ, Lin H, Wang Y, et al. High biologically effective dose radiotherapy for brain metastases may improve survival and decrease risk for local relapse among patients with small-cell lung cancer: A propensity-matching analysis. *Cancer Control* (2020) 27:1073274820936287. doi: 10.1177/1073274820936287

28. Robbins ME, Brunso-Bechtold JK, Peiffffer AM, Tsien CI, Bailey JE, Marks LB. Imaging radiation-induced normal tissue injury. *Radiat Res* (2012) 177(4):449–66. doi: 10.1667/rr2530.1

29. Fidler IJ. The biology of brain metastasis: Challenges for therapy. *Cancer J* (2015) 21(4):284–93. doi: 10.1097/PPO.0000000000000126

30. Brown JM, Giaccia AJ. The unique physiology of solid tumors: opportunities (and problems) for cancer therapy. *Cancer Res* (1998) 58(7):1408–16.

31. Hall EJ, Giaccia AJ. *Radiobiology for the radiologist*. (2011).

32. Colliez F, Fruytier AC, Magat J, Neveu MA, Cani PD, Gallez B, et al. Monitoring combretastatin A4-induced tumor hypoxia and hemodynamic changes using endogenous MR contrast and DCE-MRI. *Magn Reson Med* (2016) 75:866–72. doi: 10.1002/mrm.25642

33. Hou C, Gong G, Wang L, Su Y, Lu J, Yin Y. The study of cerebral blood flow variations during brain metastases radiotherapy. *Oncol Res Treat* (2022) 45(3):130–7. doi: 10.1159/000521291

34. Skjøtskift T, Evensen ME, Furre T, Moan JM, Amdal CD, Bogsrud TV, et al. Dose painting for re-irradiation of head and neck cancer. *Acta Oncol* (2018) 57:1693–9. doi: 10.1080/0284186X.2018.1512753

35. Chang JH, Wada M, Anderson NJ, Lim Joon D, Lee ST, Gong SJ, et al. Hypoxia-targeted radiotherapy dose painting for head and neck cancer using (18) F-FMISO PET: A biological modeling study. *Acta Oncol* (2013) 52:1723–9. doi: 10.3109/0284186X.2012.759273

36. Hendrickson K, Phillips M, Smith W, Peterson L, Krohn K, Rajendran J. Hypoxia imaging with [F-18] FMISO-PET in head and neck cancer: Potential for guiding intensity modulated radiation therapy in overcoming hypoxia-induced treatment resistance. *Radiother Oncol* (2011) 101:369–75. doi: 10.1016/j.radonc.2011.07.029

37. Neff T, Kiessling F, Brix G, Baudendistel K, Zechmann C, Giesel FL, et al. An optimized workflow for the integration of biological information into radiotherapy planning: experiences with T1w DCE-MRI. *Phys Med Biol* (2005) 50(17):4209–23. doi: 10.1088/0031-9155/50/17/020

38. Thorwarth D, Eschmann SM, Paulsen F, Alber M. Hypoxia dose painting by numbers: A planning study. *Int J Radiat Oncol Biol Phys* (2007) 68:291–300. doi: 10.1016/j.ijrobp.2006.11.061